

ORIGINAL ARTICLE

The Disconnected Brain and Executive Function Decline in Aging

Anders M. Fjell^{1,2}, Markus H. Sneve¹, Håkon Grydeland¹, Andreas B. Storsve¹ and Kristine B. Walhovd^{1,2}

¹Research Group for Lifespan Changes in Brain and Cognition, Department of Psychology, University of Oslo, Oslo 0373, Norway and ²Department of Physical Medicine and Rehabilitation, Unit of Neuropsychology, Oslo University Hospital, Oslo, Norway

Address correspondence to Anders M. Fjell, Department of Psychology, Pb. 1094 Blindern, 0317 Oslo, Norway. Email: andersmf@psykologi.uio.no

Abstract

Higher order speeded cognitive abilities depend on efficient coordination of activity across the brain, rendering them vulnerable to age reductions in structural and functional brain connectivity. The concept of “disconnected aging” has been invoked, suggesting that degeneration of connections between distant brain regions cause cognitive reductions. However, it has not been shown that changes in cognitive functions over time can be explained by simultaneous changes in brain connectivity. We followed 119 young and middle-aged (23–52 years) and older (63–86 years) adults for 3.3 years with repeated assessments of structural and functional brain connectivity and executive functions. We found unique age-related longitudinal reductions in executive function over and above changes in more basic cognitive processes. Intriguingly, 82.5% of the age-related decline in executive function could be explained by changes in connectivity over time. While both structural and functional connectivity changes were related to longitudinal reductions in executive function, only structural connectivity change could explain the age-specific decline. This suggests that the major part of the age-related reductions in executive function can be attributed to micro- and macrostructural alterations in brain connectivity. Although correlational in nature, we believe the present results constitute evidence for a “disconnected brain” view on cognitive aging.

Key words: aging, diffusion tensor imaging, executive function, functional connectivity, structural connectivity

Introduction

According to the “disconnected brain” view on cognitive aging, reductions of structural (SC) and functional connectivity (FC) contribute to cognitive decline (Ferreira and Busatto 2013; Antonenko and Floel 2014; Bennett and Madden 2014). Efficient communication between brain regions is a prerequisite for speeded higher order cognitive functions, and substantial changes in connectivity are associated with higher age (Salat et al. 2005; Antonenko and Floel 2014; Sexton et al. 2014). Speed of processing and executive functions are found to be especially related to individual differences in structural connectivity (Bennett and Madden 2014). It is therefore interesting that a major component of many theoretical frameworks of cognitive aging is the decline

of executive functions (Buckner 2004; Lustig and Jantz 2015), with the suggested neural foundation traditionally being age vulnerability of the prefrontal cortex (West 1996, 2000; Raz et al. 1997, 2005; Fjell, McEvoy, et al. 2013). Simultaneously, connections between prefrontal cortex and the basal ganglia, especially the striatum, are critical (Ward et al. 2013; Leunissen et al. 2014; Niemann et al. 2014; Rae et al. 2015). This dependency on far-reaching structural and likely functional connections makes executive functions a prima candidate to test the “disconnected brain” hypothesis of cognitive aging. However, even though the “disconnected brain” view seems like a reasonable model, we still lack convincing evidence that changes in connectivity in individual participants actually relate to reductions in executive function over time. In the present study, we address the

“disconnected brain” hypothesis model directly, by testing the degree to which longitudinal changes in executive function in younger and middle-aged versus older adults can be explained by simultaneously evolving changes in structural and functional connectivity.

To measure change in executive function, we administered a version of the Stroop task (Delis et al. 2001). Stroop is one of the most widely used measures of attentional control (MacLeod 1992), predicts age-related cognitive decline (Clark et al. 2012), and is in general sensitive to prefrontal lesions (Keifer and Tranel 2013). Large studies commonly observe increased interference effects with age on tasks such as Color-Word Interference (Delis et al. 2001) Test (Spieler et al. 1996; Van der Elst et al. 2006; Puccioni and Vallesi 2012; Adolfsdottir et al. 2014), although some have argued that this is mainly due to age-related slowing (Uttl and Graf 1997). This test includes both simpler and more complex conditions, and this enables isolation of the executive components by controlling for effects of reading and naming speed. Speed can profoundly impact the relationship between Stroop performance and brain measures (Pa et al. 2010; Adolfsdottir et al. 2014).

Several studies have related Stroop performance to FC in different populations with putative executive problems, including schizophrenia (Yan et al. 2012), Parkinson’s disease (Muller-Oehring et al. 2015), multiple sclerosis (Bonavita et al. 2015), and internet gaming disorder (Dong et al. 2015), but a consistent picture has so far not emerged. A couple of studies have reported relationships between rsFC and Stroop performance in older adults, including higher activity within medial superior parietal lobe being positively correlated with Stroop performance (Balsters et al. 2013) and the slow tail of the reaction time distribution being related to lower rsFC within the salience network (Duchek et al. 2013). It is not clear, however, whether rsFC can account for any portion of the age-expected reductions in executive functioning. An interesting subcortical structure in this respect is the putamen. Putamen has been associated with executive functions in older adults (Niemann et al. 2014), and its volume is substantially reduced with age (Walhovd et al. 2005, 2011; Fjell, Westlye, et al. 2013). FC studies have also shown that putamen connects to the frontoparietal control network, as well as other important RS networks such as the default mode network (DMN) (Choi et al. 2012). Thus, whether changes in putamen-cortical rsFC can explain executive changes, possibly in combination with cortico-cortical executive and attentional networks (Yeo et al. 2011), is an interesting question that has not been addressed.

More consistently than the rsFC results, executive function in aging has been linked to SC (Madden et al. 2009, 2012; Fjell et al. 2012) and Stroop performance specifically (Behrman-Lay et al. 2015). Of special interest, WM integrity seems to mediate the relationship between age and cognitive function (Madden et al. 2009, 2012), typically evidenced by attenuated relationships between age and cognitive function when WM integrity is controlled for (Brickman et al. 2012; Salami et al. 2012; Samanez-Larkin et al. 2012; Borghesani et al. 2013), as would be predicted from the “disconnected brain” model.

In the present study, impact of longitudinal changes in SC and FC on executive function was assessed across younger and middle-aged versus older adults. We hypothesized that changes in SC, in terms of microstructural characteristics of major WM tracts, would explain a substantial portion of the specific age-related executive changes. Although not previously tested, this hypothesis was based on findings of age reductions in SC (Salat et al. 2005; Sexton et al. 2014) and reported relationships between SC and executive function (Madden et al. 2009, 2012; Fjell et al.

2012). We segmented 8 tracts in each hemisphere and 2 commissural tracts. We further hypothesized that reductions in global WM volume would explain parts of the age-related decline in executive function. This was based on studies showing accelerated WM volume decline with age (Walhovd et al. 2011), and demonstrations of cross-sectional relationships between WM volume and different measures related to executive function (Fjell et al. 2012). For FC, we focused both on subcortical-cortical networks and targeted well-established cortico-cortical executive and attentional networks. We hypothesized that changes in FC would explain parts of the expected age-related decline in Stroop performance, based on previous studies of age effects on FC, executive performance, and the relationship between them (Madden et al. 2009, 2010, 2012). Thus, we measured rsFC between putamen and cortex, and hypothesized that changes in putamen-cortical rsFC would be related to executive changes. As a test of specificity, we tested hippocampal-cortical rsFC, where we did not expect a relationship with executive function. We also tested 2 well-established cortico-cortical executive and attentional networks (Yeo et al. 2011) consisting of 19 different seed regions distributed across the hemispheres, including orbitofrontal, middle and superior frontal, anterior cingulate, supramarginal, and temporal regions. Finally, we hypothesized, based on differing findings from mostly separate studies of FC and SC mentioned above, that contributions from SC and FS in explaining age-related variance in executive function would be complementary rather than redundant. Cortical thickness was also quantified and included as a nuisance variable in specific analyses to control for possible confounding effects on FC. Since the baseline data were acquired some time ago, a 1.5 T scanner and a BOLD scan consisting of 100 volumes were used. To assess the comparability of the results with data from the now more commonly used 3 T scanners, 44 young participants were scanned both on the 1.5 T scanner with 100 volumes and on a 3 T scanner with 150 volumes on the same day. The coherence between the network structures obtained across field strengths and scanning parameters was assessed.

Materials and Methods

Sample

The longitudinal, well-screened sample of 119 participants was drawn from the ongoing project *Cognition and Plasticity through the Lifespan* (Walhovd et al. 2014) run by the Research Group for Lifespan Changes in Brain and Cognition, Department of Psychology, University of Oslo. All procedures were approved by the Regional Ethical Committee of Southern Norway (REK-Sør), and written consent was obtained from all participants. For the first wave of data collection, participants were recruited through newspaper ads. Recruitment for the second wave was by written invitation to the original participants, with mean follow-up time of 3.3 years (SD = 0.3 years). Participants were required to be right handed, fluent Norwegian speakers, and have normal or corrected to normal vision and hearing. At both time points, participants were screened with a custom-made health interview, uncovering potential causes for exclusion, including history of injury or disease known to affect central nervous system (CNS) function, including neurological or psychiatric illness or serious head trauma, being under psychiatric treatment, use of psychoactive drugs known to affect CNS functioning, and MRI contraindications. Moreover, participants were required to score ≥ 26 on the Mini Mental State Examination (MMSE) (Folstein et al. 1975), have a Beck Depression Inventory (BDI; Beck and Steer 1987)

Table 1 Sample characteristics

	Young and middle-aged	Older adults	t	Sig
n	63	56		
Age	33.0 (23–52)	71.6 (63–86)	32.7	*
Sex (females/males)	40/24	29/27	1.3	
Education	15.9 (12–23)	16.5 (8–26)	1.1	
IQ	119 (101–133)	120 (90–146)	0.4	
MMSE	29.6 (27–30)	29.0 (26–30)	–3.9	*
Follow-up interval	3.4 (2.7–4.0)	3.1 (2.8–3.8)	–6.6	*

Note: Age, IQ, and MMSE (Mini Mental Status Exam) values from Tp2, education from Tp1. Mean (range) values are provided. Follow-up interval given in years.

*Difference between age groups is significant ($P < 0.05$).

score ≤ 16 , and obtain a normal IQ or above ($IQ \geq 85$) on the Wechsler Abbreviated Scale of Intelligence (WASI; Wechsler 1999). At both time points, all scans were evaluated by a neuroradiologist and were required to be deemed free of significant injuries or conditions. At follow-up, an additional set of inclusion criteria was employed: MMSE change from time point 1 to time point 2 $< 10\%$; California Verbal Learning Test II—Alternative Version (CVLT II; Delis et al. 2000) immediate and long delay T-score > 30 ; CVLT II immediate and long delay change from time point 1 to time point 2 $< 60\%$.

Two hundred and eighty-one participants completed Tp1 assessment. For the follow-up study, 42 opted out, 18 could not be located, 3 did not participate due to health reasons (the nature of these were not disclosed), and 3 had MRI contraindications, yielding a total of 66 dropouts (35 females, mean [SD] age = 47.3 [20.0] years). Independent samples t-tests revealed that dropouts had significantly lower FSIQ ($t = -3.92, P < 0.001$) and BDI ($t = -2.02, P = 0.046$) scores but comparable CVLT and MMSE scores ($P_s > 0.05$). More detailed dropout characteristics are published elsewhere (Storsve et al. 2014). Of the 215 participants that completed MRI and neuropsychological testing at both time points, 8 failed to meet one or more of the additional inclusion criteria for the follow-up study described above, 4 did not have adequately processed diffusion MRI data, and 2 were outliers (4 or more tracts showing change values > 6 SD from mean). This resulted in a follow-up sample of 201 participants (118 females) aged 20–84 at Tp1, see Walhovd et al. (2014). Of these, resting-state Blood-Oxygen-Level Dependent (rsBOLD) images were not acquired for the first 81, and Stroop data were missing for an additional participant, yielding a complete sample of 119, with data for both time points. Two additional participants were excluded during MRI processing. For some participants, single tracts were not reliably identified by Tracula (TRActs Constrained by UnderLying Anatomy), that is, CST (8 missing), Fmaj (6 missing), ATR right (1 missing), SLFP right (2 missing), SLFT right (1 missing), and UNC right (1 missing). Sample characteristics are provided in Table 1.

The Stroop Test

The Stroop color-word interference (CWIT) test was administered (Delis et al. 2001), consisting of the 3 traditional Stroop conditions (color naming, color name reading, interference) as well as a fourth “switching” condition. Each condition consists of 48 trials, and the participant is requested to complete all 48 trials as fast as possible. In the color condition (Stroop 1), the participant names colors from circles printed in, for example, red or blue. In the word condition (Stroop 2), the participant reads words of color names printed in black ink. In the color-word response inhibition

condition (Stroop 3), the participant names the color in which a word is presented, while ignoring the printed word. Thus, incongruence between the word’s color and identity (e.g., the word “blue” presented in red) requires inhibition and response selection. In the most complex condition, Stroop 4, the participant switches back and forth between naming the dissonant ink colors and reading the conflicting color names. Number of errors committed and number of errors committed that are corrected by the participant are registered, as well as the time taken to complete each of the 4 conditions.

MRI Acquisition and Analysis for the Longitudinal data

Imaging data were collected using a 12-channel head coil on a 1.5 T Siemens Avanto scanner (Siemens Medical Solutions, Erlangen, Germany) at Rikshospitalet, Oslo University Hospital. The same scanner and sequences were used at both time points, and the sequences had the following parameters:

For Morphometry

The pulse sequence used for morphometric analyses included 2 repetitions of a 160 slices sagittal T_1 -weighted magnetization prepared rapid gradient echo (MPRAGE) sequences with the following parameters: repetition time (TR)/echo time (TE)/time to inversion (TI)/flip angle = 2400 ms/3.61 ms/1000 ms/8°, matrix = 192 × 192, field of view (FOV) = 240, voxel size = 1.25 × 1.25 × 1.20 mm, scan time 4 min 42 s.

For Structural Connectivity

Diffusion-weighted MRI (dMRI) was performed using a single-shot twice-refocused spin-echo echo planar imaging pulse sequence optimized to minimize eddy current-induced distortions (primary slice direction, axial; phase encoding direction, columns; TR = 8200 ms; TE = 82 ms; voxel size = 2.0 mm isotropic; number of slices = 64; FOV = 256; matrix size = 128 × 128 × 64; b value = 700 s/mm²; number of diffusion encoding gradients directions = 30; number of $b = 0$ images = 10; number of acquisitions = 2). Acquisition time was 11 min 21 s.

For Functional Connectivity

The resting-state BOLD sequence included 28 transversally oriented slices (no gap), measured using a BOLD-sensitive T_2^* -weighted EPI sequence (TR = 3000 ms, TE = 70 ms, flip angle = 90°, voxel size = 3.44 × 3.44 × 4 mm, FOV = 220, descending acquisition, GRAPPA acceleration factor = 2), producing 100 volumes and lasting for approximately 5 min. Three dummy volumes were collected at the start to avoid T_1 saturation effects.

Image processing and analyses of FC and atrophy were performed at the Neuroimaging Analysis Laboratory, Research Group for Lifespan Changes in Brain and Cognition, Department of Psychology, University of Oslo, while DTI analyses were run at the Martinos Center for Biomedical Imaging, Harvard Medical School, Boston. To ensure coherence in the processing across the different imaging modalities, all imaging modalities were processed within the general FreeSurfer environment with the addition of some custom-made procedures for processing of the functional connectivity data.

Morphometry

Morphometric analyses were performed by use of FreeSurfer v. 5.1 (<http://surfer.nmr.mgh.harvard.edu/>) (Dale et al. 1999; Fischl et al. 1999, 2002; Fischl and Dale 2000), see a detailed account elsewhere (Walhovd et al. 2014). All volumes were inspected for accuracy and minor manual edits were performed

when needed by a trained operator on the baseline images, usually restricted to removal of nonbrain tissue included within the cortical boundary. The cross-sectionally processed images were subsequently run through the longitudinal stream in FreeSurfer (Reuter et al. 2012), with high sensitivity and robustness as well as inverse consistency (Reuter et al. 2010; Reuter and Fischl 2011). In addition, probabilistic methods (temporal fusion) were applied to further reduce the variability across time points. These procedures were also used to calculate the total volume of WM T_1 hypointensities.

Functional Connectivity

Resting-state functional imaging data were pre-processed following LCBC's custom analysis stream. Images were motion corrected, slice timing corrected, and smoothed (5 mm FWHM) in volume space using FSL's FMRI Expert Analysis Tool (FEAT; <http://fsl.fmrib.ox.ac.uk/fsl/fslwiki>). Then, FSL's Multivariate Exploratory Linear Optimized Decomposition into Independent Components (MELODIC) was used in combination with FMRIB's ICA-based Xnoiseifier (FIX) to auto-classify independent components into "good" and "bad" components and remove the bad components from the 4D fMRI data (Salimi-Khorshidi et al. 2014). FreeSurfer-defined individually estimated anatomical masks of cerebral white matter (WM) and cerebrospinal fluid/lateral ventricles (CSF) were resampled to each individual's functional space. All anatomical voxels that "constituted" a functional voxel had to be labeled as WM or CSF for that functional voxel to be considered a functional representation of noncortical tissue. Average time series were then extracted from functional WM and CSF voxels, and were regressed out of the FIX-cleaned 4D volume together with a set of estimated motion parameters (rotation/translation) and their derivatives. Following recent recommendations about noise removal from resting-state data (Hallquist et al. 2013), we band-pass filtered the data (0.009–0.08 Hz) after regression of confound variables.

FC was calculated seed based for subcortical and cortical networks. First, FC from putamen and hippocampus was calculated separately as the correlation between the average time series of all voxels within each structure and every vertex in the ipsilateral cerebral hemispheres, each correlation being variance-stabilized using the Fisher z-transformation (Silver and Dunlap 1987), yielding 2 FC maps for each participant for each hemisphere. The rsFC value that was later used in the multi-modal analyses was the mean rsFC between putamen and the vertices showing an age interaction in the relationship between Stroop change and rsFC change (see below). To calculate FC within established cortical functional networks, we took advantage of Yeo et al. (2011) cortical parcellation estimated by intrinsic functional connectivity from 1000 participants and made available in FreeSurfer's average surface space (http://surfer.nmr.mgh.harvard.edu/fswiki/CorticalParcellation_Yeo2011). This is among the best validated delineations of cortical resting-state networks. The parcellation scheme consists of 17 networks in each hemisphere as well as values representing the estimated confidence of each surface vertex belonging to its assigned network. Spheres (6 dilations around center vertex; 127 vertices) were drawn on the average surface around each network's highest confidence vertex (vertices of a network consisted of several disconnected segments), resampled into individual subject space, and the mean activity among these 127 vertices was correlated with all other vertices. Two networks were targeted, representing executive and attentional networks (networks 8 and 13, Fig. 1). One such rsFC map was created for each node within a network, and the mean of all maps belonging to the nodes of a given network was then calculated. This map

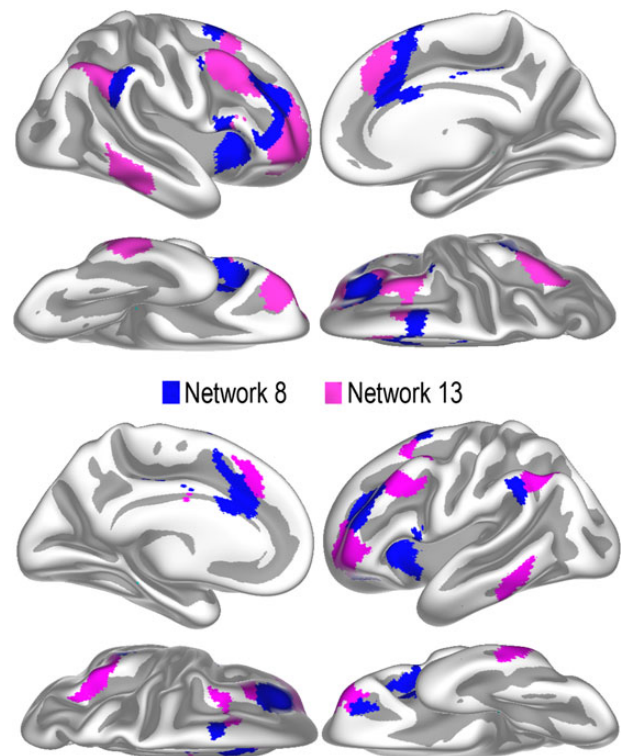


Figure 1. Executive and attentional networks. Two cortical networks were chosen based on the cortical parcellation from Yeo et al. (2011), both can generally be referred to as attentional and executive networks, although consensus has not been reached on the exact delineation of such networks. More specifically, following the divisions of Power et al. (2011), the pink (Network 8 from Yeo et al.) overlaps with a frontal-parietal task control system, and the blue with a salience system. Alternatively, Network 8 can be said to partly represent a cingulo-opercular network while Network 13 contains major parts of a frontoparietal control network. FC was calculated between each of the nodes belonging to each of the networks, imposed on our data from the parcellation scheme from Yeo et al. Top panel: Right hemisphere. Bottom panel: Left hemisphere.

represented the rsFC map for that particular network. This was done separately for Network 8 and Network 13 in the Yeo et al. parcellation scheme, and vertex-wise analyses were run testing the relationship between rsFC change and Stroop change for each vertex on the brain surface. Surface maps of mean rsFC for each network were entered into the statistical analyses, and separate analyses were also run for the maps from individual nodes separately.

Structural Connectivity

For dMRI analyses, TRActs Constrained by UnderLying Anatomy (TRACULA), part of FreeSurfer, was used to delineate major WM tracts of interest (TOI) (Yendiki et al. 2011). This is a novel algorithm for automated global probabilistic tractography that estimates the posterior probability of each pathway given the dMRI data. The posterior probability is decomposed into a data likelihood term, which uses the "ball-and-stick" model of diffusion (Behrens et al. 2007), and a pathway prior term, which incorporates prior anatomical knowledge on the pathways from a set of training subjects. The segmentation labels required by TRACULA were obtained by processing the T_1 -weighted images of the study subjects with the automated cortical parcellation and subcortical segmentation tools in FreeSurfer (Fischl et al. 2002; Fischl, Salat, et al. 2004; Fischl, van der Kouwe, et al. 2004). The longitudinal stream of TRACULA used here is specifically designed to

reconstruct tracts jointly from longitudinal diffusion data, using a subject's data from all time points jointly (Yendiki et al. 2016). This is a rather unique approach, designed to ensure point-to-point correspondence between the tracts reconstructed at different time points, while eliminating any bias toward any single time point. A further advantage of using a tractography approach such as TRACULA is that we alleviate the need for inter-subject registrations, since the tracts are delineated without relying on subject registration, which could increase sensitivity if there are anatomical differences between subjects. In addition to the commissural tracts Forceps Major (Fmaj) and Minor (Fmin), the following tracts were segmented in each hemisphere: the anterior thalamic radiation (ATR), cingulum angular bundle (CAB), cingulum-cingulum bundle (CCG), cortico-spinal tract (CST), inferior longitudinal fasciculus (ILF), superior longitudinal fasciculus, temporal part (SLFT), superior longitudinal fasciculus, parietal part (SLFP), and the uncinate fasciculus (UNC).

As head motion has previously been shown to produce spurious findings in diffusion MRI studies (Yendiki et al. 2013), care was taken to control for head motion in the present study. To quantify head motion in each scan, we derived volume-by-volume translation and rotation from the affine registration, as well as slice-by-slice signal dropout measures that are specific to DW-MRI (Benner et al. 2011). The registration-based measures are better at capturing slower, between-volume motion, whereas the intensity-based measures are better at capturing more rapid, within-volume motion. The total motion index was computed from these measures, as described in Yendiki et al. (2013), and used as covariate in statistical analyses.

MRI Acquisition and Analysis for the Longitudinal Data

In addition to the main longitudinal analyses, 44 healthy young participants were scanned on 1.5 T and 3 T scanners on the same day at follow-up (mean age: 23.1 years, range: 20.1–26.6 years, 24 females). The rationale was to test whether the network structure obtained by the 1.5 T scanner was replicable on a 3 T scanner with a higher number of volumes. The 1.5 T scanner and sequence were identical to those used in the longitudinal analyses. For 3 T, imaging was performed with a Siemens Skyra 3 T whole-body MRI unit equipped with a 24-channel Siemens head coil (Siemens Medical Systems). For the resting-state functional imaging scan, 43 transversally oriented slices (no gap) were measured using a BOLD-sensitive T_2^* -weighted EPI sequence (repetition time [TR] = 2390 ms, echo time [TE] = 30 ms, flip angle = 90°, voxel size = 3 × 3 × 3 mm, field of view [FOV] = 224 × 224 mm, interleaved acquisition, GRAPPA acceleration factor = 2). At the start of the fMRI run, 3 dummy volumes were collected to avoid T_1 saturation effects in the analyzed data. The resting-state fMRI run produced 150 volumes and thus lasted approximately 6 min which has been shown to be sufficient to produce stable connectivity measures (Van Dijk et al. 2010). Anatomical T_1 -weighted MPRAGE images consisting of 176 sagittally oriented slices were obtained using a turbo field echo pulse sequence (TR = 2300 ms, TE = 2.98 ms, flip angle = 8°, voxel size = 1 × 1 × 1 mm, FOV = 256 × 256 mm). These scans underwent the same preprocessing steps as those reported above, using the 17 networks solution from Yeo et al. as template, with each vertex weighted by the confidence of it being a part of its assigned network.

Statistical Analyses

Longitudinal changes in brain measures derived from each imaging modality (FC, SC, WM volume, cortical thickness) were

quantified as the difference of each measure between time points. Follow-up interval was included as covariate of no interest in all analyses, and movement during scanning was included as additional nuisance variables for the neuroimaging analyses. In analyses where age group was not a variable of interest, age was also included as covariate. For SC, WM volume, and thickness, analyses were done on TOIs or regions-of-interest (ROIs). For FC, vertex-wise analyses on the cortical surface were run with general linear models (GLM) implemented in FreeSurfer. Results were tested against an empirical null distribution of maximum cluster size across 10 000 iterations using Z Monte Carlo simulations (Hayasaka and Nichols 2003; Hagler et al. 2006), synthesized with a cluster-forming threshold of $P < 0.05$ (2-sided), yielding clusters corrected for multiple comparisons across the surface. Change values from these clusters were then extracted and used in multi-modal analyses together with the other TOI/ROI measures.

First, all Stroop variables were correlated with age, cross-sectionally at each time point as well as change over time. An age function was fitted to each variable by use of generalized additive mixed models (GAMM) in R (www.r-project.org), run through the PING data portal (Bartsch et al. 2014), yielding an optimal fit to both the cross-sectional and the longitudinal information. Akaike Information Criterion (AIC) (Akaike 1974) and the Bayesian Information Criterion (BIC) were used to guide model selection and help guard against over-fitting. Since basic common cognitive processes, such as processing speed, are shared between the 4 Stroop conditions, a multiple regression analysis with age as dependent and change in each Stroop time variable as simultaneous predictors was run to test whether the expected increase in the Stroop interference effect in the complex condition could be statistically explained by changes in more fundamental processes. Variable(s) uniquely related to age was then chosen for further testing against neuroimaging measures.

Second, effects of age on the relationship between FC change and Stroop 4 change were tested by comparing the slopes for the FC-memory relationships between age groups. Stroop 1 and 2 times were included as covariates. Values from significant clusters were extracted for post hoc plotting of observed effects and for inclusion in multi-modal multiple regression analyses. Analyses were run for putamen-cortical rsFC and hippocampal-cortical rsFC. Similar analyses were run for the 2 cortical executive and attentional networks.

Third, testing of Stroop 4 change against change in SC was done by partial correlations. Since we did not have any hypotheses of hemispheric effects, mean values across hemispheres were used in the analyses. P values were corrected by a factor of 30 (3 diffusion metrics [FA, RD, MD] × 10 tracts), adjusted for the correlations between the dependent variables, according to the procedure described here, <http://www.quantitativeskills.com/sisa/calculations/bonfer.htm>. Analyses were first run without age included as covariate and were then repeated controlling for age. Also, analyses were run both with and without the other Stroop change variables as covariates. Correlation coefficients were compared between the young and middle-aged versus the old group by t-testing of Fisher's z-transformed correlation coefficients. We also tested the relationship between T_1 hypointensities and Stroop 4 change, and re-run the above DTI-Stroop analyses while controlling for the possible confounding influence of hypointensities.

Finally, a series of multiple regressions were run with Stroop 4 change as the dependent variable, where age, significant variables from the SC and FC analyses, as well as the different Stroop 1–3 change parameters were systematically included and excluded to assess how the relationship between age and Stroop 4

Table 2 Stroop performance and relationship to age

	Young and middle-aged, n = 63		Older, n = 56		Age correlation		
	Tp1	Tp2	Tp1	Tp2	Tp1	Tp2	Tp2/Tp1
Stroop 1 color	27.1 (4.5)	25.8 (3.4)	33.0 (4.7)	31.8 (6.0)	0.52 [^]	0.54 [^]	0.09
Stroop 2 words	21.0 (3.7)	19.9 (3.0)	22.7 (3.9)	22.3 (3.5)	0.22 [*]	0.37 [^]	0.21 [*]
Stroop 3 color/words	44.8 (8.8)	42.5 (6.7)	59.9 (11.5)	60.1 (15.2)	0.58 [^]	0.62 [^]	0.20 [*]
Stroop 4 shifting	50.6 (9.5)	48.1 (10.7)	65.2 (14.1)	70.4 (22.9)	0.54 [^]	0.61 [^]	0.37 [^]

Note: For the ratio between time points, Tp2/Tp1, partial correlations with age were run controlling for interval between time points.

^{*}P < 0.05.

[^]P < 0.001.

was mediated by the different connectivity variables. We followed the recommendations from a recent review (Bennett and Madden 2014), by

1. Assessing age–cognition relationships with and without controlling for the connectivity measures (test of the so-called “brain-mediating model”)
2. Assessing connectivity–cognition relationships after controlling for age-related variance (test of for the so-called “independent variable model”)

It is argued that such an approach gives more compelling evidence regarding the nature of relationships among age, brain, and cognitive variables than testing the performance of single models in isolation (Bennett and Madden 2014). Also, we followed the strategy outlined in Hedden et al. to estimate the proportion of age-related variance shared with a given connectivity measure, by use of the formula $(r_{A-C}^2 - r_{A-C \times Bk}^2) / r_{A-C}^2$, where each *k*th connectivity measure, that is, brain marker (B), was partialled from the correlation between age (A) and executive function, that is, cognitive function (C) (Hedden et al. 2016). Further, to estimate unique age-related variance shared with each connectivity measure (Bk), by use of the formula $(r_{A-C \times B \in k}^2 - r_{A-C \times B \in k}^2) / r_{A-C}^2$, where (B \in k) is the set of all connectivity measures and (B \notin k) is the set of all connectivity measures excluding the *k*th measure.

Results

Stroop Performance

Age correlated positively with Stroop time at both time points for all conditions, with the highest correlations for the 2 complex conditions, Stroops 3 and 4 ($r = 0.53$ to 0.62 , $P < 0.001$) (Table 2 and Fig. 2). Due to practice effects, the young and middle-aged group showed significantly faster completion of all conditions at Tp2 compared with Tp1 ($P < 0.05$). For the older group, significant improvement in Stroop 1 (color) was seen ($P < 0.05$), along with a significant increase in Stroop 4 (shifting) ($P < 0.05$).

Age was associated with relative increase in time to completion of the task from Tp1 to Tp2 in all conditions but Stroop 1, with effect sizes of $r = 0.21$, $P < 0.05$, (Stroop 2), 0.20 , $P < 0.05$, (Stroop 3), and 0.37 , $P < 0.001$ (Stroop 4). Proportion change in each condition was then entered into a multiple regression, along with follow-up interval, with age as dependent variable. Stroop 4 ($\beta = 0.29$, $t = 3.77$, $P < 0.0005$) was the only change variable demonstrating a unique relationship with age when all other variables were controlled for and was therefore selected for further analyses.

Structural Connectivity

Change in Stroop 4 was correlated with annualized percent change in FA, MD, and RD in 10 tracts, as well as total volume

of T_1 hypointensities, with motion and interval included as covariates (Table 3). Many relationships were found at an uncorrected α -level of 0.05. Mean absolute correlation between each metric was 0.41, yielding an α -level of 0.007 corrected for multiple comparisons. Stroop 4 correlations with ILF MD ($r = 0.27$) and SLFT MD ($r = 0.28$) survived the corrected threshold. Rate of change in WM hypointensities and Stroop 4 change correlated at $r = 0.24$ ($P = 0.009$), and positive correlations at trend level were found at both time points (Tp1 $r = 0.17$, $P = 0.07$ /Tp2 $r = 0.10$, $P = 0.04$). The significant correlations between DTI and Stroop 4 change were therefore re-run with WM hypointensities at both time points as covariates. The DTI correlations survived inclusion of WM hypointensities as covariates (ILF MD $r = 0.23$; SLFT MD $r = 0.23$). Next, age was included as an additional covariate. The correlation with ILF MD change was still significant ($r = 0.23$), also when controlling for hypointensities ($r = 0.22$). This correlation was re-run with change in Stroop1 and 2 as additional covariates, and the relationship was still significant ($r = 0.22$ and $r = 0.20$ when controlling for hypointensities). The Stroop–SC correlation was not significantly different between young and middle-aged versus older adults ($r = 0.34$ vs 0.15 for young/middle-aged and older, respectively).

Functional Connectivity

We tested the relationship between putamen-cortical rsFC change and Stroop 4 vertex-wise, with age, movement, interval, and change in Stroop 1 and 2 as covariates. No significant relationships were seen. Separate analyses run for younger/middle-aged and older adults, with age within each group regressed out, showed significant effects (Fig. 3). In the right hemisphere, a cluster of 4991 mm² was found in the young and middle-aged group, peaking in the lingual gyrus, and 1 cluster of 3750 mm² in the left hemisphere was found in the old group, peaking in superior parietal cortex. When tested directly, age group had widespread effects on the relationship between rsFC and Stroop 4 change, mainly in medial posterior cortical areas across hemispheres, including lingual gyrus, cuneus, and fusiform cortex (Fig. 4, see [Supplementary Information](#) for details of the significant clusters). This interaction was due to increases in time needed to fulfill the task being related to decreased in rsFC in the group of older adults (partial $\beta = 0.26$, $P < 0.05$), while the opposite relationship was found in the young and middle-aged group (partial $\beta = -0.30$, $P < 0.05$) (Fig. 5), yielding significantly different regression slopes ($P < 0.005$). Almost identical age interactions were found in the contralateral hemisphere (Fig. 6). As a test of specificity, the analyses were run for rsFC between hippocampus and the rest of the cortex, with no significant results.

The relationship between rsFC change in each of the 2 executive and attentional cortical networks and Stroop changes was tested with identical procedures. No age interactions survived

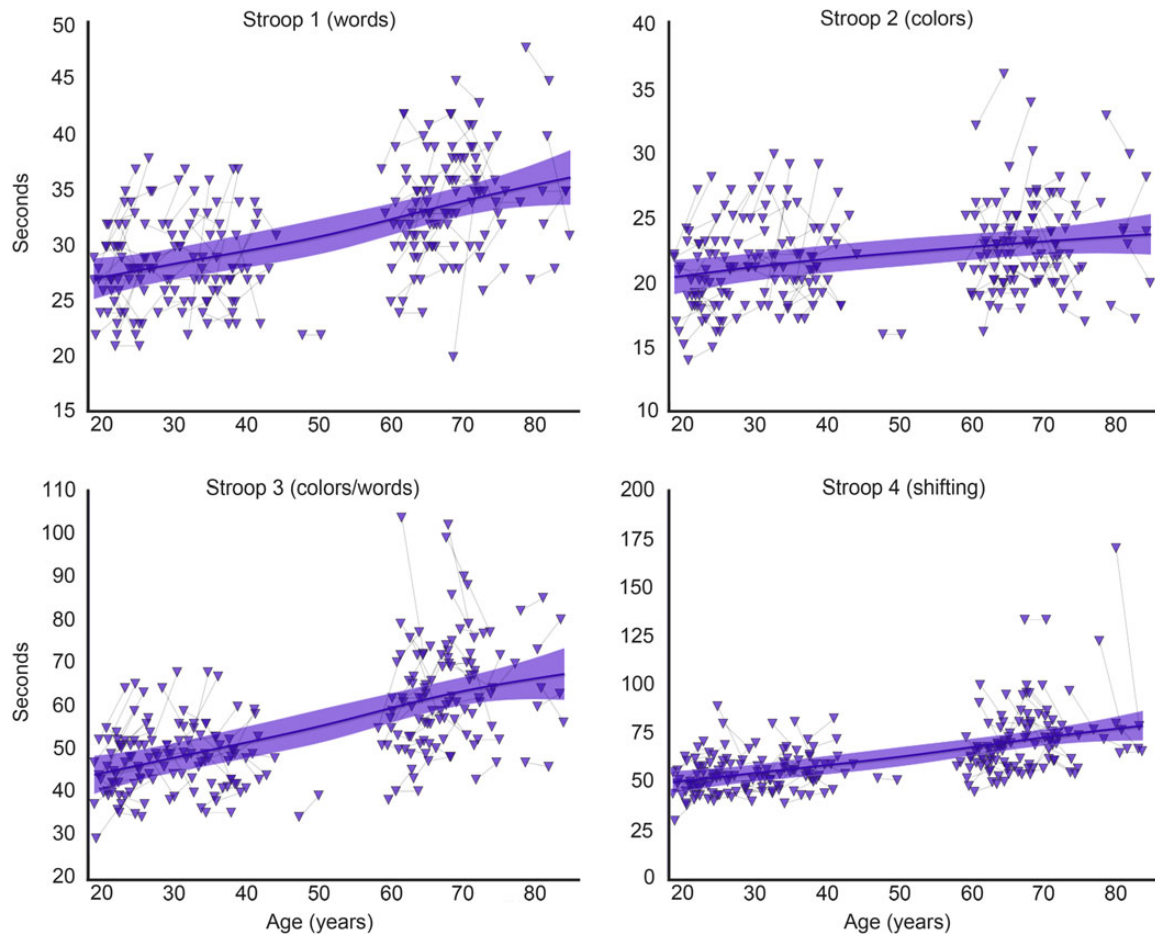


Figure 2. Longitudinal changes in Stroop completion time with age. Each Stroop condition was fitted to age by use of generalized additive mixed models (GAMM), yielding the optimal fit by taking advantage of both the cross-sectional and the longitudinal information.

Table 3 Correlations between Stroop 4 change and structural connectivity change

	Δ MD	Δ RD	Δ FA
ATR	0.10	0.09	-0.11
CAB	0.15	0.15	-0.09
CCG	0.25	0.26	-0.20
CST	0.23	0.19	-0.06
Fmajor	0.24	0.14	0.05
Fminor	-0.01	-0.02	0.00
ILF	0.27^a	0.23	-0.12
SLFT	0.28	0.21	-0.04
SLFP	0.22	0.19	-0.07
UNC	0.21	0.21	-0.16

Note: Motion change during scanning was included as covariate. Italicized variables represent surviving corrections for multiple comparisons. Bold indicates $P < 0.05$.

ATR, anterior thalamic radiation; CAB, Cingulum angular bundle; CCG, Cingulum-cingulum bundle; CST, Cortico-spinal tract; Fmaj, Forceps Major; Fmin, Forceps Minor; ILF, Inferior longitudinal fasciculus; SLFT, superior longitudinal fasciculus, temporal part; SLFP, superior longitudinal fasciculus, parietal part; UNC, uncinata fasciculus.

^aSurviving corrections for age.

permutation testing. Inspection of the uncorrected P value maps revealed a pattern of results for Network 8 that was highly similar to the putamen results. We therefore repeated the age interaction

analyses for each of the nodes of this network separately (5 in left and 4 in right hemisphere). For 3 nodes in the left and 2 nodes in the right hemisphere, change in rsFC between the node and the rest of the cortex was differently related to Stroop change in each age group (corrected for multiple comparisons across space) (Fig. 7, see [Supplementary Information](#) for details on the significant clusters). The direction of effects was identical to the putamen results, that is, increased rsFC was related to prolonged completion time in younger and middle-aged with the opposite relationship seen in older adults. However, since the results from the main analysis with total rsFC change within the whole network did not survive proper corrections, we did not perform other follow-up analyses on the cortical networks, and only the putamen results were used in the following multi-modal analyses.

Multi-Modal Analyses

A series of multiple regression analyses were run to test the optimal linear combination of different variables in explaining Stroop 4 change. In all models, follow-up interval and age were entered in the first step. This first step yielded $\beta = 0.44$ ($P < 0.00005$) for age, and a correlation between the model and Stroop 4 change of $r = 0.38$ (adjusted $R^2 = 0.13$, $F_{2,116} = 90.68$, $P < 0.0005$). In the next model, Stroops 1, 2, and 3 were entered simultaneously, slightly reducing β for age to $=0.39$ ($P < 0.0005$). In addition, Stroop 3 was marginally significant ($\beta = 0.17$, $P = 0.067$), while Stroops 1 and 2

were not ($P > 0.30$). When the analysis was re-run without Stroops 1 and 2, Stroop 3 yielded a significant contribution beyond age ($\beta = 0.20$, $P < 0.05$). Thus, Stroop 3 was kept in the model for the multi-modal connectivity analyses. Since Stroops 1 and 2 were not significantly related to Stroop 4 when the variance shared with Stroop 3 was accounted for, these variables were not

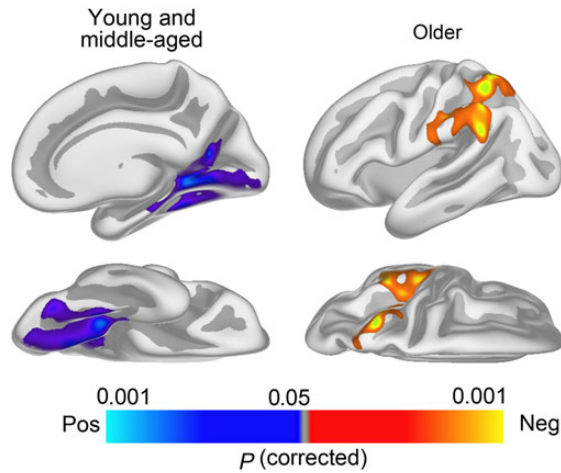


Figure 3. Relationship between putamen-cortical rsFC and Stroop 4 completion time. GLMs were run testing the relationship between change in rsFC between putamen and the cortex and change in Stroop 4 completion time, with interval, Stroop 1 and Stroop 2 change, movement during scanning and within-group age included as nuisance variables. Analyses were run in each age group separately, revealing a relationship between increased rsFC and reduced Stroop 4 completion time in the old group, and the opposite relationship in the young and middle-aged. The results are corrected for multiple comparisons across space by Monte Carlo simulations and projected onto semi-inflated surface models for better visualization.

included in the next models, with Stroop 3 then accounting for variance associated with Stroops 1 and 2 such as speed and visuo-perceptual skills.

In the next model, ILF MD change was added together with mean rsFC change in the clusters showing significant age interactions depicted in Figure 4, along with the interaction term of age and rsFC. Movement during scanning was also added as covariates in all neuroimaging analyses. Age was significant ($\beta = 0.35$, $P < 0.005$), as was Stroop 3 ($\beta = 0.21$, $P < 0.05$), ILF MD change ($\beta = 0.24$, $P < 0.01$), while the interaction of rsFC and age was marginally significant ($\beta = 0.15$, $P = 0.080$). The analysis was re-run without Stroop 3 included, and now the P value of the age \times rsFC interaction term was significant ($\beta = 0.18$, $P < 0.05$). In this model with movement parameters, interval, age, ILF MD change, rsFC change, and rsFC \times age, we found that age, ILD MD change, and rsFC \times age contributed significantly, and the full model correlated 0.48 with Stroop 4 change (adjusted $R^2 = 0.17$, $F_{9,109} = 3.58$, $P < 0.001$). Adding Stroop 1 and Stroop 2 conditions as additional covariates did not render any of these variables not significant. To test whether the rsFC effect could be explained by atrophy, cortical thickness reduction was extracted from an overlapping region of the cortex, consisting of lingual gyrus, fusiform gyrus, and cuneus across hemispheres, and included as an additional covariate. This did not affect the unique contribution from the age \times rsFC interaction ($\beta = 0.18$, $P < 0.05$). Since there could be potential structural compensatory mechanisms in aging manifesting in thickness effects in different regions, Stroop 4 change was correlated with thickness change across 34 regions covering the entire cortex. For the medial orbitofrontal ($r = -0.20$, $P < 0.05$) and parahippocampal ($r = -0.24$, $P < 0.01$) cortex, significant correlations were found, but these would not survive proper multiple comparison corrections.

Finally, we tested how much of the variance in Stroop 4 change that could be explained by an optimal linear combination

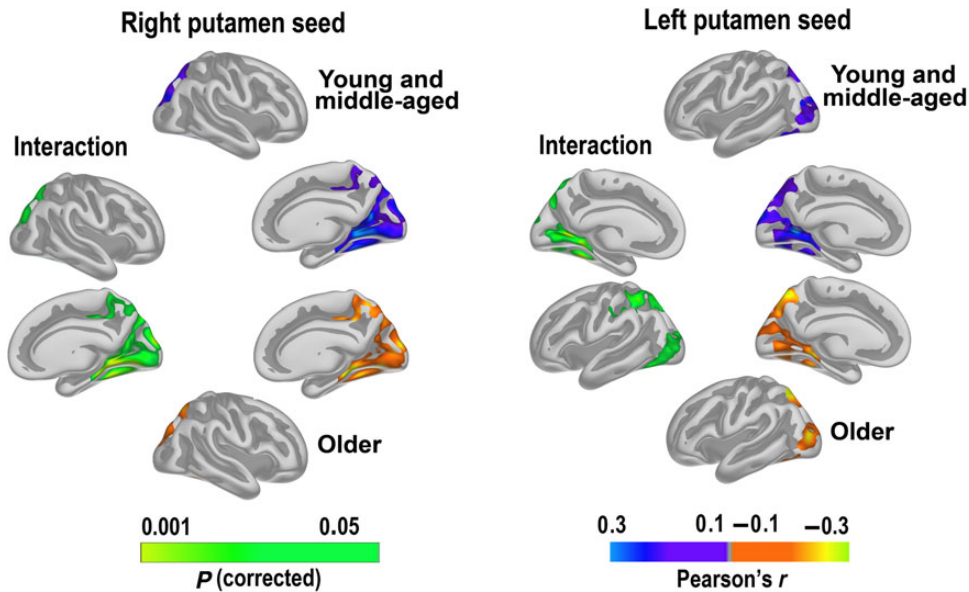


Figure 4. Effects of age on the relationship between ipsilateral putamen-cortical rsFC and Stroop 4 completion time. Change in rsFC between putamen and the ipsilateral cerebral cortex was correlated with change in Stroop4 completion time, with Stroop1 and Stroop2 change, interval between tests, movement at both time points, and within-group age included as covariates of no interest. Interaction maps are in green-yellow and represent regions where the relationship between rsFC and Stroop change differed as a function of age group. Maps are corrected for multiple comparisons across space by Monte Carlo simulations and projected onto semi-inflated surface models for better visualization. Corresponding Pearson correlation maps in orange-green (older group) and blue-purple (young and middle-aged group) are shown for illustrative purposes, masked by the group interaction effect. In the older group, relatively higher rsFC over time was related to relatively faster Stroop 4 completion, with the opposite pattern in the young and middle-aged group.

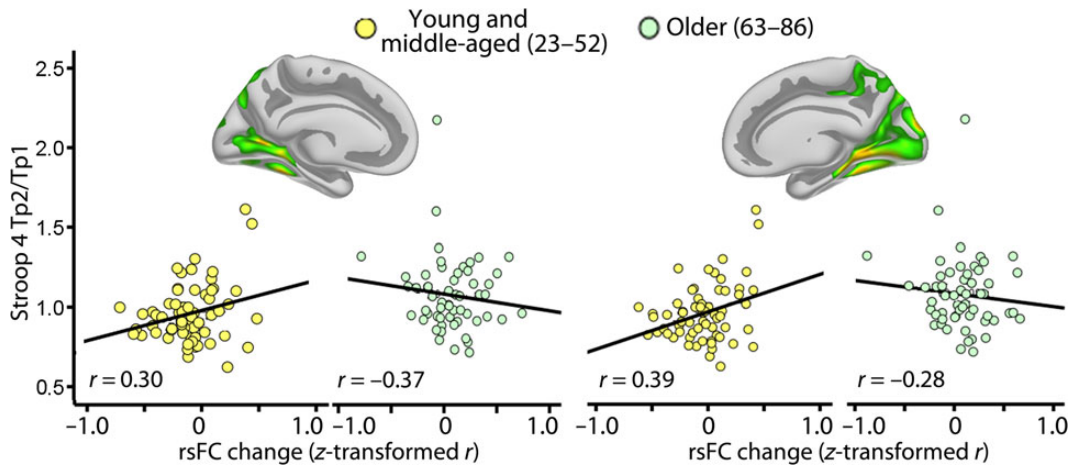


Figure 5. Scatterplots of age-dependent rsFC–Stroop 4 relationships. rsFC changes from all vertices showing a significant age interaction were extracted and correlated with Stroop 4 change for each age group separately to illustrate the age-dependent relationship. r -values are obtained with Stroop1 and Stroop2 change, interval between tests, movement at both time points, and within-group age partialled out.

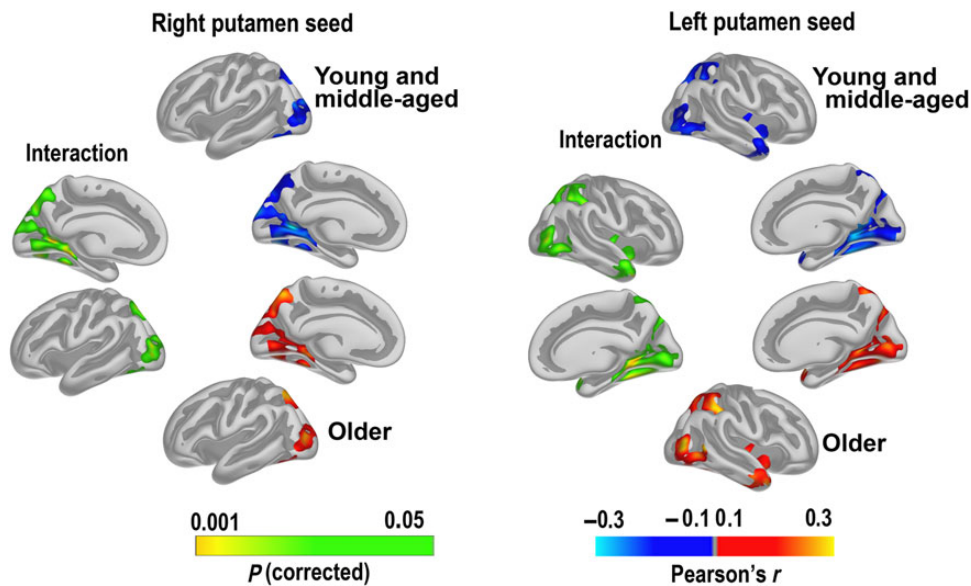


Figure 6. Effects of age on the relationship between contralateral putamen–cortical rsFC and Stroop 4 completion time. Same as Figure 4, but rsFC calculated from the contralateral putamen.

of the imaging parameters alone. To avoid the problem of multi-collinearity among WM tracts, all tracts and parameters in Table 3 that were significantly ($P < 0.05$, uncorrected) related to Stroop 4 when age was not regressed out were entered into a principal component analysis (PCA) to extract 1 principal component (PC). This component explained 57.3% of the variance in change among these tracts (see [Supplementary Information](#)). Age, interval, movement, the DTI PC, rsFC, and its age interaction term were entered in a multiple regression analysis with the PCA as dependent variable. We also entered total WM volume change. Age ($\beta = 0.31$, $P < 0.10$) and the DTI PC term were marginally significant ($\beta = 0.16$, $P < 0.10$), while WM volume change ($\beta = -0.28$, $P < 0.005$) and the rsFC \times age term was significant ($\beta = 0.17$, $P < 0.05$). In total, this model correlated 0.50 with Stroop 4 change (adjusted $R^2 = 0.21$, $F_{6,112} = 6.21$, $P < 0.00005$).

In none of the analyses reported above did any of the covariates of no interest (interval, movement) yield contributions approaching significance (all P s > 0.2).

Mediation Analyses

Based on the relationships between a series of partial correlations, we calculated how much of the age variance in Stroop 4 that could be attributed to each of the neuroimaging variables (Hedden et al. 2016) (see SI). In total, 82.5% of the age variance in Stroop 4 change could be accounted for by change in SC, rsFC, and WM volume. Performing the calculations for each measure separately yielded 66.5% shared variance for age and WM volume in explaining Stroop change, 37.8% for age and DTI PC, and 0.0% for age and rsFC. Further, 15.3% of the age variance in Stroop explained by WM volume was shared with DTI, while

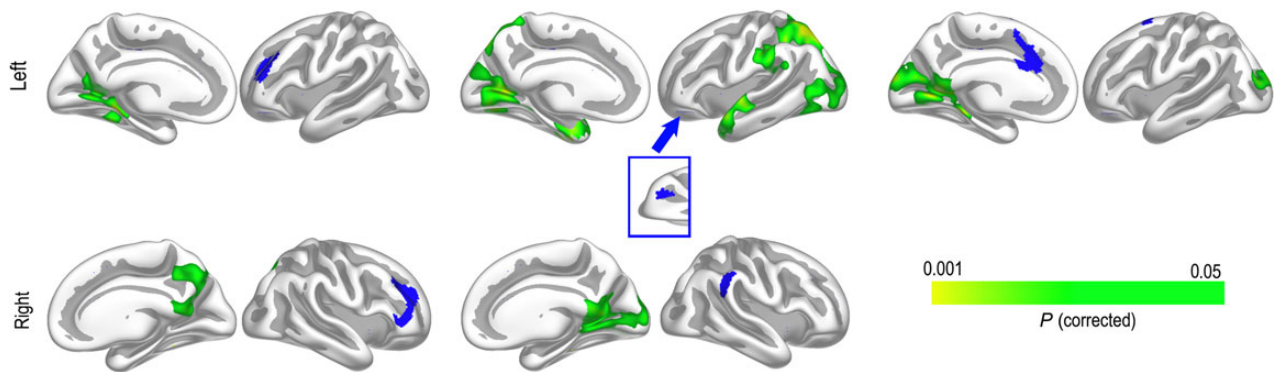


Figure 7. Effects of age on the relationship between ipsilateral cortical network rsFC and Stroop 4 completion time. Same as Figure 4, but seed points were cortical parcellations belonging to validated executive/attentional networks identified in Yeo et al. (2011) and illustrated in Figure 1. No significant effects survived corrections when each network was tested as a whole, but significant age interactions were seen for selected regions within Network 8. The seed regions are shown in blue. The direction of effects is identical to the putamen results (Fig. 4).

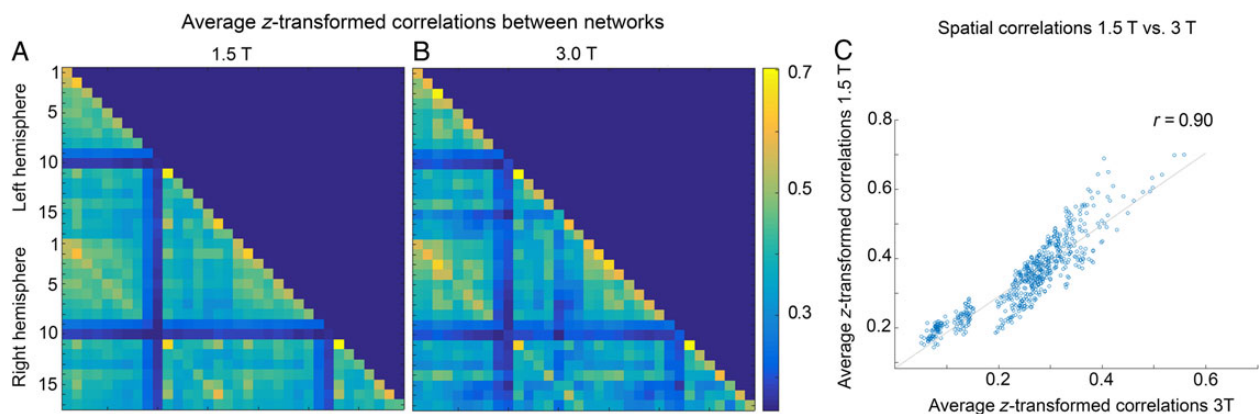


Figure 8. Replication of network structure across field strengths and acquisitions. To assess coherence in network structure between the 1.5 T 100 volume sequence used for the longitudinal analyses and a 3 T 150 volume sequence, 44 young healthy participants were scanned on both scanners on the same day. As can be seen by comparing plots A (1.5 T) and B (3 T), the spatial relationship between networks was very similar across field strength and sequence. Panel C shows the direct relationship between coherence for each network, with the spatial correlation being $r = 0.90$.

the amount of age variance in Stroop explained by DTI and shared with WM volume was 44.6%.

1.5 T vs 3 T Validation Analyses

Forty-four healthy young participants were scanned on 1.5 T with 100 volumes and on a 3 T with 150 volumes on the same day. Within- and between-network functional connectivity was analyzed for 1.5 T data and 3 T data separately. Group averaged 1.5 T and 3 T network correlation values, z-transformed using Fisher's method, are presented in Figure 8 (A and B). As can be seen, the internetwork organization appears to be almost identical across field strength. This was confirmed by a formal test, revealing a spatial correlation between the plots in panel A and B of $r = 0.90$, illustrated by the scatterplot in panel C of Figure 8. In conclusion, the global connectivity pattern estimated from the 1.5 T data and the 3 T data was very similar.

Discussion

According to the “disconnected brain” model, degeneration of structural and functional brain connections cause cognitive reductions in aging, but convincing longitudinal evidence has been lacking. Here we demonstrate that age-specific longitudinal

decline in executive performance, that is, inhibition and switching costs, was related to reduced connectivity in aging. Executive decline was greater than what could be attributed to change in basic, speeded cognitive processes, and the major part of the age-related decline was explained by the connectivity markers. Although correlational in nature, the results support the “disconnected brain” view of cognitive aging (Bennett and Madden 2014). Validation analyses demonstrated excellent convergence between network structure detected across 1.5 and 3 T scanners, which is encouraging for longitudinal studies where baseline scans often date several years back.

The “Disconnected Brain” and Age-Related Decline of Executive Function

Putamen-cortical rsFC, diffusion-based SC as well as WM volume contributed to explain executive function changes independently of age. Compellingly, however, 82.5% of the age-related reductions in executive function could be explained by the connectivity measures combined. Thus, the present results indicate that measures related to connectivity can account for a substantial proportion of age-related decline in executive function, in line with the “disconnected brain” view on aging. Since higher cognitive functions depend on efficient inter-regional communication, even subtle

reductions of structural and functional aspects of inter-regional connections could have detrimental effects. Executive functions contribute to coordination of activity across a wide range of cortical and subcortical brain structures, which would make them vulnerable to reduced communication efficiency. The present demonstration that changes in connectivity can explain most of the age-related decline in executive function supports this line of reasoning. Some specificity was also seen, in that change in rsFC between the hippocampus and the rest of the cortex was not related to executive function. Instead, previous studies have shown relationships between hippocampal rsFC change and memory (Fjell et al. 2016), hippocampal atrophy and memory (Fjell, McEvoy, et al. 2013) as well as between limbic tract integrity and pattern separation performance (Bennett et al. 2015).

Importantly, the 3 classes of connectivity markers were largely complementary in explaining age-independent executive function changes, which would be similar to the linear decline in a cross-sectional study. However, only the 2 structural markers explained unique parts of the age-related variance in executive change, which would be similar to a nonlinear addition to a cross-sectional linear decline. While age had a profound effect on the relationship between executive function and putamen-cortical rsFC, rsFC did not explain any of the age variance in Stroop decline. This is in line with 1 previous study (Hedden et al. 2016), but fits less well with a second, in which FC but not SC significantly accounted for a portion of the age-related variance in semantic categorization (Madden et al. 2010). Comparable to the present results, a recent study found that 75% of the age-related cross-sectional variance in executive function could be explained by a set of brain markers, but in contrast to the present longitudinal results, most of this variance was shared between brain markers (Hedden et al. 2016). We observed shared variance between different classes of brain measures, but there was also substantial variance in age-related executive decline that was not shared between connectivity measures.

Structural Connectivity Changes and Executive Function

In addition to the combined effect of the different connectivity measures, interesting observations were made also regarding the specific measures. For instance, although mean diffusion change in only 2 tracts survived proper statistical corrections for multiple comparisons, there was modest anatomical specificity, as the correlations were comparable in magnitude across many tracts, and trends were found also for tracts not assumed specifically important for executive functions. The PCA revealed that 57.3% of the variation in change in DTI metrics across tracts could be explained by a single component, which was significantly related to executive function. This is in line with a previous study showing that a principal component accounted for the shared variance between DTI and reaction time (Penke et al. 2010), and it is not clear whether tract-specific effects can be expected over and above the general state of the WM microstructure (Bennett and Madden 2014). We also observed that age accounted for a substantial part of the shared variance between microstructural changes in tracts and Stroop performance changes. This observation is partly in line with the so-called independent variable model (Bennett and Madden 2014), according to which relationships between brain variables and cognition can be explained by their common relationship to age. Similar results were seen in some other studies that directly contrasted the independent variable model relative to a brain-mediation model and concluded that relationships between WM integrity and cognition

were reduced or no longer significant after controlling for the influence of age (Zahr et al. 2009; Salami et al. 2012; Borghesani et al. 2013). Still, relationships between DTI parameters and cognitive function have often survived corrections for the influence of age (for reviews, see Madden et al. (2012); Bennett and Madden (2014)), and the age-independent relationship between ILF and executive function in the present study also shows that all the relationships were not entirely mediated by age. Interestingly, ILF connects the occipital lobe to more anterior brain regions, especially the temporal lobes. Projections of ILF tract ending into the cortex show overlap with the rsFC effects, indicating anatomical correspondence between DTI-based SC and fMRI-based FC changes.

Although a correlation of 0.24 was observed between T_1 WM hypointensity volume and Stroop 4 change, hypointensity volume could not account for the DTI–Stroop relationships. Vascular factors are known to impact WM integrity in aging (Bender and Raz 2015) and also cognitive function (Lopez-Oloriz et al. 2014; Meier et al. 2014; Staals et al. 2015). Here we used T_1 hypointensities as a proxy for effects of cerebrovascular disease on WM structure, and the robustness of the present results to the inclusion of T_1 WM hypointensities could mean that cerebrovascular factors do not account for all the variance between WM integrity change and change in executive performance. However, this question needs to be further tested with more thorough analysis of T_2 -weighted MRI images to accurately quantify the effects of the total load of different cerebrovascular conditions, including lobar microbleeds, lacunes, WM hyperintensities, and perivascular spaces (Staals et al. 2015).

WM volume change also predicted change in Stroop performance independently of age. WM volume and DTI measures are modestly correlated (Fjell et al. 2008) and follow partly different trajectories through life (Westlye et al. 2010), although they both have been related to cognitive control functions (Fjell et al. 2012). This partial independence between DTI and WM volumetric measures makes them relevant to jointly include in multimodal analyses. WM volume change yielded the strongest unique contributions to explain change in executive function. Importantly, although DTI and volumetric measures shared some of the age variance in executive change, neither measure was redundant. Actually, 44.6% of the age variance in Stroop explained by DTI was shared with WM volume, and only 15.3% of the variance explained by volume was explained by DTI, mimicking the results of a previous cross-section study (Fjell et al. 2012).

Functional Connectivity Changes and Executive Function

Relationships between putamen-cortical rsFC and executive function were found within each age group, with the age interactions constituting the most compelling finding, demonstrating that age can be an important mediator of the relationship between cognitive function and brain connectivity. Although no effects survived corrections for the whole network analysis, several regions that are part of executive FC networks showed age interactions in predicting executive change. Previous studies have shown both age-related increases and decreases in FC, with implications for cognition depending on the specific nature of the network and the type of cognitive function in question (Ferreira and Busatto 2013; Antonenko and Floel 2014). Thus, with regard to FC, it seems that the “disconnected brain” model has some merit, but that the relationships between FC and cognition vary in a manner that is not easy to predict based on this model alone. In fact, the relationship between FC and cognition appears rather unpredictable, and more work is required before this

measure becomes a useful tool for describing the aging brain. The relevance of striatal-cortical circuits for cognitive changes in aging has also previously been proposed (Howard and Howard 2013). Interestingly, effects were seen in regions related to processing of visual information, which have been observed in previous rsFC studies using versions of the Stroop task (Zysset et al. 2007; Polk et al. 2008). Similar regions of effect were found for the putamen-cortical analyses and in the cortical network analyses, indicating that changes in how these posterior cortices communicate with different cortical and subcortical regions may be of importance for age-related changes in executive function, at least as indexed by the Stroop task. One can speculate that increased FC between putamen and posterior cortices may be more beneficial for older than younger and middle-aged adults, related to interactions between increased executive demands and visual processing demands during the complex color-word switching condition for the older adults. It can also be noted that the basal ganglia is hypothesized to be important for connections between posterior cortical areas and prefrontal cortex related to automatic behavior (Helie et al. 2014).

A limitation of the study is the low sampling density in the middle-aged range. This caused the young and middle-aged group to have a rather wide age range, and we could not create a third group of middle-aged adults only. Higher sampling density in the middle-age range would allow better modeling of the observed break point between young and older. For the rsFC–executive function relationship, we assume that the positive relationship in young participants would be followed by no relationship or a weak relationship in a group of middle-aged only, before a negative relationship would be seen for the group of older adults. Testing this would be interesting, but requires higher sampling density in the middle age range. In addition, although longitudinal data were available for all, the total sample size was only 119. A larger sample or more longitudinal data points for each participant would yield more power to detect effects also for rsFC. Still, sample size was sufficient to detect effects of SC measures, suggesting that rsFC is not a very strong predictor of age-related decline in executive function. Further, the BOLD sequence included only 100 volumes. However, the validation analyses in an independent sample showed robust delineation of the same networks as those obtained with 150 volumes on a 3 T scanner.

Conclusion

The results of the present longitudinal study indicate unique age-related reductions in executive function as indexed by changes in Stroop 4 performance over and above changes in more basic, speeded cognitive processes. Importantly, 82.5% of the age-related variance in executive change could be explained by the full set of connectivity variables. This was due to partly shared and partly unique variance explained by the 2 structural measures—DTI and WM volume. While rsFC also was related to executive change, this relationship was highly mediated by age. Also of interest, age-related executive change did not primarily have a frontal basis, but seemed to be affected by disconnectivity in different brain regions and networks, including in putamen-occipital and frontal-occipital rsFC. An inherent limitation in all aging studies, whether they are longitudinal or cross-sectional, is that age and time cannot be experimentally manipulated, yielding results that by necessity are correlational. Direct causal inferences between brain connectivity and executive function are therefore not valid. Still, as we observe both age-dependent and age-independent relationships between connectivity change and

executive function change, we believe the results make probable that brain aging affects executive function through reductions of connectivity at more than 1 level, in general coherence with the “disconnected brain” view on cognitive aging.

Supplementary Material

Supplementary material can be found at: <http://www.cercor.oxfordjournals.org/>.

Funding

This work was supported by the Department of Psychology, University of Oslo (to K.B.W. and A.M.F.), the Norwegian Research Council (to K.B.W. and A.M.F.), the US-Norway Fulbright Foundation (to A.B.S.) and the project has received funding from the European Research Council’s Starting Grant scheme under grant agreements 283634 (to A.M.F.) and 313440 (to K.B.W.).

Notes

Conflict of Interest: None declared.

References

- Adolfsson S, Haasz J, Wehling E, Ystad M, Lundervold A, Lundervold AJ. 2014. Salient measures of inhibition and switching are associated with frontal lobe gray matter volume in healthy middle-aged and older adults. *Neuropsychology*. 28:859–869.
- Akaike H. 1974. A new look at the statistical model identification. *IEEE Trans Automat Contr*. 19:716–723.
- Antonenko D, Floel A. 2014. Healthy aging by staying selectively connected: a mini-review. *Gerontology*. 60:3–9.
- Balsters JH, O’Connell RG, Galli A, Nolan H, Greco E, Kilcullen SM, Bokde AL, Lai R, Upton N, Robertson IH. 2013. Changes in resting connectivity with age: a simultaneous electroencephalogram and functional magnetic resonance imaging investigation. *Neurobiol Aging*. 34:2194–2207.
- Bartsch H, Thompson WK, Jernigan TL, Dale AM. 2014. A web-portal for interactive data exploration, visualization, and hypothesis testing. *Front Neuroinformatics*. 8:25.
- Beck AT, Steer R. 1987. Beck depression inventory scoring manual. New York: The Psychological Corporation.
- Behrens TE, Berg HJ, Jbabdi S, Rushworth MF, Woolrich MW. 2007. Probabilistic diffusion tractography with multiple fibre orientations: what can we gain? *Neuroimage*. 34:144–155.
- Behrman-Lay AM, Usher C, Conturo TE, Correia S, Laidlaw DH, Lane EM, Bolzenius J, Heaps JM, Salminen LE, Baker LM, et al. 2015. Fiber bundle length and cognition: a length-based tractography MRI study. *Brain Imaging Behav*. 9 (4):765–775.
- Bender AR, Raz N. 2015. Normal-appearing cerebral white matter in healthy adults: mean change over 2 years and individual differences in change. *Neurobiol Aging*. 36:1834–1848.
- Benner T, van der Kouwe AJ, Sorensen AG. 2011. Diffusion imaging with prospective motion correction and reacquisition. *Magn Resonance Med*. 66:154–167.
- Bennett IJ, Huffman DJ, Stark CE. 2015. Limbic tract integrity contributes to pattern separation performance across the lifespan. *Cereb Cortex*. 25:2988–2999.
- Bennett IJ, Madden DJ. 2014. Disconnected aging: cerebral white matter integrity and age-related differences in cognition. *Neuroscience*. 276:187–205.

- Bonavita S, Sacco R, Della Corte M, Esposito S, Sparaco M, d'Ambrosio A, Docimo R, Bisecco A, Lavorgna L, Corbo D, et al. 2015. Computer-aided cognitive rehabilitation improves cognitive performances and induces brain functional connectivity changes in relapsing remitting multiple sclerosis patients: an exploratory study. *J Neurol*. 262:91–100.
- Borghesani PR, Madhyastha TM, Aylward EH, Reiter MA, Swamy BR, Schaie KW, Willis SL. 2013. The association between higher order abilities, processing speed, and age are variably mediated by white matter integrity during typical aging. *Neuropsychologia*. 51:1435–1444.
- Brickman AM, Meier IB, Korgaonkar MS, Provenzano FA, Grieve SM, Siedlecki KL, Wasserman BT, Williams LM, Zimmerman ME. 2012. Testing the white matter retrogenesis hypothesis of cognitive aging. *Neurobiol Aging*. 33:1699–1715.
- Buckner RL. 2004. Memory and executive function in aging and AD: multiple factors that cause decline and reserve factors that compensate. *Neuron*. 44:195–208.
- Choi EY, Yeo BT, Buckner RL. 2012. The organization of the human striatum estimated by intrinsic functional connectivity. *J Neurophysiol*. 108:2242–2263.
- Clark LR, Schiehser DM, Weissberger GH, Salmon DP, Delis DC, Bondi MW. 2012. Specific measures of executive function predict cognitive decline in older adults. *J Int Neuropsychol Soc*. 18:118–127.
- Dale AM, Fischl B, Sereno MI. 1999. Cortical surface-based analysis. I. Segmentation and surface reconstruction. *Neuroimage*. 9:179–194.
- Delis D, Kaplan E, Kramer JH. 2001. Delis-Kaplan executive function system: technical manual. San Antonio (TX): Harcourt Assessment Company.
- Delis DC, Kramer JH, Kaplan E, Ober BA. 2000. California verbal learning test - second edition (CVLT - II). San Antonio (TX): The Psychological Corporation.
- Dong G, Lin X, Potenza MN. 2015. Decreased functional connectivity in an executive control network is related to impaired executive function in Internet gaming disorder. *Prog Neuropsychopharmacol Biol Psychiatry*. 57:76–85.
- Duchek JM, Balota DA, Thomas JB, Snyder AZ, Rich P, Benzinger TL, Fagan AM, Holtzman DM, Morris JC, Ances BM. 2013. Relationship between Stroop performance and resting state functional connectivity in cognitively normal older adults. *Neuropsychology*. 27:516–528.
- Ferreira LK, Busatto GF. 2013. Resting-state functional connectivity in normal brain aging. *Neurosci Biobehav Rev*. 37:384–400.
- Fischl B, Dale AM. 2000. Measuring the thickness of the human cerebral cortex from magnetic resonance images. *Proc Natl Acad Sci USA*. 97:11050–11055.
- Fischl B, Salat DH, Busa E, Albert M, Dieterich M, Haselgrove C, van der Kouwe A, Killiany R, Kennedy D, Klaveness S, et al. 2002. Whole brain segmentation: automated labeling of neuroanatomical structures in the human brain. *Neuron*. 33:341–355.
- Fischl B, Salat DH, van der Kouwe AJ, Makris N, Segonne F, Quinn BT, Dale AM. 2004. Sequence-independent segmentation of magnetic resonance images. *Neuroimage*. 23(Suppl. 1):S69–S84.
- Fischl B, Sereno MI, Dale AM. 1999. Cortical surface-based analysis. II: Inflation, flattening, and a surface-based coordinate system. *Neuroimage*. 9:195–207.
- Fischl B, van der Kouwe A, Destrieux C, Halgren E, Segonne F, Salat DH, Busa E, Seidman LJ, Goldstein J, Kennedy D, et al. 2004. Automatically parcellating the human cerebral cortex. *Cereb Cortex*. 14:11–22.
- Fjell AM, McEvoy L, Holland D, Dale AM, Walhovd KB. Alzheimer's Disease Neuroimaging I. 2013. Brain changes in older adults at very low risk for Alzheimer's disease. *J Neurosci*. 33:8237–8242.
- Fjell AM, Sneve MH, Storsve AB, Grydeland H, Yendiki A, Walhovd KB. 2016. Brain events underlying episodic memory changes in aging: a longitudinal investigation of structural and functional connectivity. *Cereb Cortex*. 26(3):1272–1286.
- Fjell AM, Westlye LT, Amlien IK, Walhovd KB. 2012. A multimodal investigation of behavioral adjustment: post-error slowing is associated with white matter characteristics. *Neuroimage*. 61:195–205.
- Fjell AM, Westlye LT, Greve DN, Fischl B, Benner T, van der Kouwe AJ, Salat D, Bjornerud A, Due-Tonnessen P, Walhovd KB. 2008. The relationship between diffusion tensor imaging and volumetry as measures of white matter properties. *Neuroimage*. 42:1654–1668.
- Fjell AM, Westlye LT, Grydeland H, Amlien I, Espeseth T, Reinvang I, Raz N, Holland D, Dale AM, Walhovd KB, Alzheimer Disease Neuroimaging I. 2013. Critical ages in the life course of the adult brain: nonlinear subcortical aging. *Neurobiol Aging*. 34:2239–2247.
- Folstein MF, Folstein SE, McHugh PR. 1975. Mini-mental state: a practical method for grading the cognitive state of patients for the clinician. *J Psychiatr Res*. 12:189–198.
- Hagler DJ Jr, Saygin AP, Sereno MI. 2006. Smoothing and cluster thresholding for cortical surface-based group analysis of fMRI data. *Neuroimage*. 33:1093–1103.
- Hallquist MN, Hwang K, Luna B. 2013. The nuisance of nuisance regression: spectral misspecification in a common approach to resting-state fMRI preprocessing reintroduces noise and obscures functional connectivity. *Neuroimage*. 82:208–225.
- Hayasaka S, Nichols TE. 2003. Validating cluster size inference: random field and permutation methods. *Neuroimage*. 20:2343–2356.
- Hedden T, Schultz AP, Rieckmann A, Mormino EC, Johnson KA, Sperling RA, Buckner RL. 2016. Multiple brain markers are linked to age-related variation in cognition. *Cereb Cortex*. 26(4):1388–1400.
- Helie S, Ell SW, Ashby FG. 2014. Learning robust cortico-cortical associations with the basal ganglia: An integrative review. *Cortex*. 64C:123–135.
- Howard JH Jr, Howard DV. 2013. Aging mind and brain: is implicit learning spared in healthy aging? *Front Psychol*. 4:817.
- Keifer E, Tranel D. 2013. A neuropsychological investigation of the Delis-Kaplan Executive Function System. *J Clin Exp Neuropsychol*. 35:1048–1059.
- Leunissen I, Coxon JP, Caeyenberghs K, Michiels K, Sunaert S, Swinnen SP. 2014. Subcortical volume analysis in traumatic brain injury: the importance of the fronto-striato-thalamic circuit in task switching. *Cortex*. 51:67–81.
- Lopez-Oloriz J, Lopez-Cancio E, Arenillas JF, Hernandez M, Dorado L, Dacosta-Aguayo R, Barrios M, Soriano-Raya JJ, Miralbell J, Bargallo N, et al. 2014. Diffusion tensor imaging, intracranial vascular resistance and cognition in middle-aged asymptomatic subjects. *Cerebrovasc Dis*. 38:24–30.
- Lustig C, Jantz T. 2015. Questions of age differences in interference control: when and how, not if? *Brain Res*. 1612:59–69.
- MacLeod CM. 1992. The Stroop task: the “gold standard” of attentional measures. *J Exp Psychol*. 121:12–14.
- Madden DJ, Bennett IJ, Burzynska A, Potter GG, Chen NK, Song AW. 2012. Diffusion tensor imaging of cerebral white

- matter integrity in cognitive aging. *Biochim Biophys Acta*. 1822:386–400.
- Madden DJ, Bennett IJ, Song AW. 2009. Cerebral white matter integrity and cognitive aging: contributions from diffusion tensor imaging. *Neuropsychol Rev*. 19:415–435.
- Madden DJ, Costello MC, Dennis NA, Davis SW, Shepler AM, Spaniol J, Bucur B, Cabeza R. 2010. Adult age differences in functional connectivity during executive control. *Neuroimage*. 52:643–657.
- Meier IB, Gu Y, Guzman VA, Wiegman AF, Schupf N, Manly JJ, Luchsinger JA, Viswanathan A, Martinez-Ramirez S, Greenberg SM, et al. 2014. Lobar microbleeds are associated with a decline in executive functioning in older adults. *Cerebrovasc Dis*. 38:377–383.
- Muller-Oehring EM, Sullivan EV, Pfefferbaum A, Huang NC, Poston KL, Bronte-Stewart HM, Schulte T. 2015. Task-rest modulation of basal ganglia connectivity in mild to moderate Parkinson's disease. *Brain Imaging Behav*. 9(3):619–638.
- Niemann C, Godde B, Staudinger UM, Voelcker-Rehage C. 2014. Exercise-induced changes in basal ganglia volume and cognition in older adults. *Neuroscience*. 281C:147–163.
- Pa J, Possin KL, Wilson SM, Quitania LC, Kramer JH, Boxer AL, Weiner MW, Johnson JK. 2010. Gray matter correlates of set-shifting among neurodegenerative disease, mild cognitive impairment, and healthy older adults. *J Int Neuropsychol Soc*. 16:640–650.
- Penke L, Munoz Maniega S, Murray C, Gow AJ, Hernandez MC, Clayden JD, Starr JM, Wardlaw JM, Bastin ME, Deary IJ. 2010. A general factor of brain white matter integrity predicts information processing speed in healthy older people. *J Neurosci*. 30:7569–7574.
- Polk TA, Drake RM, Jonides JJ, Smith MR, Smith EE. 2008. Attention enhances the neural processing of relevant features and suppresses the processing of irrelevant features in humans: a functional magnetic resonance imaging study of the Stroop task. *J Neurosci*. 28:13786–13792.
- Power JD, Cohen AL, Nelson SM, Wig GS, Barnes KA, Church JA, Vogel AC, Laumann TO, Miezin FM, Schlaggar BL, et al. 2011. Functional network organization of the human brain. *Neuron*. 72:665–678.
- Puccioni O, Vallesi A. 2012. Conflict resolution and adaptation in normal aging: the role of verbal intelligence and cognitive reserve. *Psychol Aging*. 27:1018–1026.
- Rae CL, Hughes LE, Anderson MC, Rowe JB. 2015. The prefrontal cortex achieves inhibitory control by facilitating subcortical motor pathway connectivity. *J Neurosci*. 35:786–794.
- Raz N, Gunning FM, Head D, Dupuis JH, McQuain J, Briggs SD, Loken WJ, Thornton AE, Acker JD. 1997. Selective aging of the human cerebral cortex observed in vivo: differential vulnerability of the prefrontal gray matter. *Cereb Cortex*. 7:268–282.
- Raz N, Lindenberger U, Rodrigue KM, Kennedy KM, Head D, Williamson A, Dahle C, Gerstorf D, Acker JD. 2005. Regional brain changes in aging healthy adults: general trends, individual differences and modifiers. *Cereb Cortex*. 15:1676–1689.
- Reuter M, Fischl B. 2011. Avoiding asymmetry-induced bias in longitudinal image processing. *Neuroimage*. 57:19–21.
- Reuter M, Rosas HD, Fischl B. 2010. Highly accurate inverse consistent registration: a robust approach. *Neuroimage*. 53:1181–1196.
- Reuter M, Schmansky NJ, Rosas HD, Fischl B. 2012. Within-subject template estimation for unbiased longitudinal image analysis. *Neuroimage*. 61:1402–1418.
- Salami A, Eriksson J, Nilsson LG, Nyberg L. 2012. Age-related white matter microstructural differences partly mediate age-related decline in processing speed but not cognition. *Biochim Biophys Acta*. 1822:408–415.
- Salat DH, Tuch DS, Greve DN, van der Kouwe AJ, Hevelone ND, Zaleta AK, Rosen BR, Fischl B, Corkin S, Rosas HD, et al. 2005. Age-related alterations in white matter microstructure measured by diffusion tensor imaging. *Neurobiol Aging*. 26:1215–1227.
- Salimi-Khorshidi G, Douaud G, Beckmann CF, Glasser MF, Griffanti L, Smith SM. 2014. Automatic denoising of functional MRI data: combining independent component analysis and hierarchical fusion of classifiers. *Neuroimage*. 90:449–468.
- Samanez-Larkin GR, Levens SM, Perry LM, Dougherty RF, Knutson B. 2012. Frontostriatal white matter integrity mediates adult age differences in probabilistic reward learning. *J Neurosci*. 32:5333–5337.
- Sexton CE, Walhovd KB, Storsve AB, Tamnes CK, Westlye LT, Johansen-Berg H, Fjell AM. 2014. Accelerated changes in white matter microstructure during aging: a longitudinal diffusion tensor imaging study. *J Neurosci*. 34:15425–15436.
- Silver N, Dunlap W. 1987. Averaging correlation coefficients: should Fisher's z-transformation be used? *J Appl Psychol*. 72:1979–1981.
- Spieler DH, Balota DA, Faust ME. 1996. Stroop performance in healthy younger and older adults and in individuals with dementia of the Alzheimer's type. *J Exp Psychol Hum Percept Performance*. 22:461–479.
- Staals J, Booth T, Morris Z, Bastin ME, Gow AJ, Corley J, Redmond P, Starr JM, Deary IJ, Wardlaw JM. 2015. Total MRI load of cerebral small vessel disease and cognitive ability in older people. *Neurobiol Aging*. 36:2806–2811.
- Storsve AB, Fjell AM, Tamnes CK, Westlye LT, Overbye K, Aasland HW, Walhovd KB. 2014. Differential longitudinal changes in cortical thickness, surface area and volume across the adult life span: regions of accelerating and decelerating change. *J Neurosci*. 34(25):8488–8498.
- Uttl B, Graf P. 1997. Color-Word Stroop test performance across the adult life span. *J Clin Exp Neuropsychol*. 19:405–420.
- Van der Elst W, Van Boxtel MP, Van Breukelen GJ, Jolles J. 2006. The Stroop color-word test: influence of age, sex, and education; and normative data for a large sample across the adult age range. *Assessment*. 13:62–79.
- Van Dijk KR, Hedden T, Venkataraman A, Evans KC, Lazar SW, Buckner RL. 2010. Intrinsic functional connectivity as a tool for human connectomics: theory, properties, and optimization. *J Neurophysiol*. 103:297–321.
- Walhovd KB, Fjell AM, Reinvang I, Lundervold A, Dale AM, Eilertsen DE, Quinn BT, Salat D, Makris N, Fischl B. 2005. Effects of age on volumes of cortex, white matter and subcortical structures. *Neurobiol Aging*. 26:1261–1270; discussion 1275–1268.
- Walhovd KB, Storsve AB, Westlye LT, Drevon CA, Fjell AM. 2014. Blood markers of fatty acids and vitamin D, cardiovascular measures, body mass index, and physical activity relate to longitudinal cortical thinning in normal aging. *Neurobiol Aging*. 35:1055–1064.
- Walhovd KB, Westlye LT, Amlien I, Espeseth T, Reinvang I, Raz N, Agartz I, Salat DH, Greve DN, Fischl B, et al. 2011. Consistent neuroanatomical age-related volume differences across multiple samples. *Neurobiol Aging*. 32:916–932.
- Ward P, Seri AS, Cavanna AE. 2013. Functional neuroanatomy and behavioural correlates of the basal ganglia: evidence from lesion studies. *Behav Neurol*. 26:219–223.

- Wechsler D. 1999. Wechsler abbreviated scale of intelligence. San Antonio (TX): The Psychological Corporation.
- West RL. 1996. An application of prefrontal cortex function theory to cognitive aging. *Psychol Bull.* 120:272–292.
- West R. 2000. In defense of the frontal lobe hypothesis of cognitive aging. *J Int Neuropsychol Soc.* 6:727–729; discussion 730.
- Westlye LT, Walhovd KB, Dale AM, Bjornerud A, Due-Tønnessen P, Engvig A, Grydeland H, Tamnes CK, Ostby Y, Fjell AM. 2010. Life-span changes of the human brain white matter: diffusion tensor imaging (DTI) and volumetry. *Cereb Cortex.* 20:2055–2068.
- Yan H, Tian L, Yan J, Sun W, Liu Q, Zhang YB, Li XM, Zang YF, Zhang D. 2012. Functional and anatomical connectivity abnormalities in cognitive division of anterior cingulate cortex in schizophrenia. *PLoS ONE.* 7:e45659.
- Yendiki A, Koldewyn K, Kakunoori S, Kanwisher N, Fischl B. 2013. Spurious group differences due to head motion in a diffusion MRI study. *Neuroimage.* 88C:79–90.
- Yendiki A, Panneck P, Srinivasan P, Stevens A, Zollei L, Augustinack J, Wang R, Salat D, Ehrlich S, Behrens T, et al. 2011. Automated probabilistic reconstruction of white-matter pathways in health and disease using an atlas of the underlying anatomy. *Front Neuroinformatics.* 5:23.
- Yendiki A, Reuter M, Wilkens P, Rosas HD, Fischl B. 2016. Joint reconstruction of white-matter pathways from longitudinal diffusion MRI data with anatomical priors. *Neuroimage.* 127:277–286.
- Yeo BT, Krienen FM, Sepulcre J, Sabuncu MR, Lashkari D, Hollinshead M, Roffman JL, Smoller JW, Zollei L, Polimeni JR, et al. 2011. The organization of the human cerebral cortex estimated by intrinsic functional connectivity. *J Neurophysiol.* 106:1125–1165.
- Zahr NM, Rohlfing T, Pfefferbaum A, Sullivan EV. 2009. Problem solving, working memory, and motor correlates of association and commissural fiber bundles in normal aging: a quantitative fiber tracking study. *Neuroimage.* 44:1050–1062.
- Zysset S, Schroeter ML, Neumann J, von Cramon DY. 2007. Stroop interference, hemodynamic response and aging: an event-related fMRI study. *Neurobiol Aging.* 28:937–946.